A 47 % Fractional Bandwidth Sequential Power Amplifier with High Back-off Efficiency

Sarmad Ozan, Alex Pitt, Manish Nair, Mark A. Beach and Tommaso Cappello
Communication Systems & Networks Research Group, University of Bristol, United Kingdom
{s.ozan, alex.pitt, manish.nair, m.a.beach, tommaso.cappello}@bristol.ac.uk

***Abstract*—This paper presents a 2.9-4.7 GHz sequential power amplifier (SPA) based on two 10 W GaN high electron mobility transistors (HEMTs). A wideband combiner and an input splitter which establish an optimal relative phase for achieving the maximum efficiency are designed. The proposed SPA attains a bandwidth between 2.9 GHz and 4.7 GHz (47 % fractional bandwidth) with efficiency enhancement at output power back-off (OPBO). The measured results over the band of operation show a drain efficiency of 43 % - 56 % at maximum output power of 40 dBm - 42 dBm, and of 36 % - 52 % at 6 dB OPBO.**

***Index Terms*—Efficiency enhancement, peak-to-average power ratio (PAPR), phase compensation, sequential power amplifier (SPA), wideband.**

I. Introduction

THE contemporary fifth-generation (5G) of communication systems necessitates novel radio frequency (RF) front ends that linearly amplifies high peak-to-average power ratio (PAPR) waveforms over a wide bandwidth with high efficiency and stable output power. To realise such stringent requirements, RF power amplifiers (PAs) delivering high efficiencies across PAPRs ranging from at least 6 dB up to 12 dB are required. This is because 5G waveforms present PAPRs of such values [1], which degrades the PA efficiency. On the other hand, a PA attains its peak efficiency at the peak output power, and so its average efficiency varies depending on the PAPR. Peak efficiency also needs to be maintained over the PA bandwidth which is particularly challenging.

Several efficiency enhancement schemes are investigated at large output power back-off (OPBO) levels; commonly encountered when amplifying high PAPR waveforms. These include envelope tracking (ET) [2], outphasing [3], and Doherty PA (DPA) [4]. The leading solution for base-station transmitters is currently the DPA. This is mainly due to the fact that it has a single RF-input which allows the 'upgrade' of existing transmitter PAs easy to do. The DPA, widely used for delivering high efficiencies at peak power levels and OPBO, comprises of two constituent PAs, known as the 'carrier' PA and the 'peaking' PA, with active load modulation. However, the classical DPA approach remains band-limited because of the utilisation of quarter-wave transmission lines for impedance transformation which also aids in active load modulation. This despite the adoption of bandwidth improvement methods such as parallel impedance transformation [5] or dual-frequency matching [6].

This work is funded by EPSRC CDT in Communications EP/L016656/1 with research affiliated to EPSRC Prosperity Partnership SWAN (EP/T005572/1).

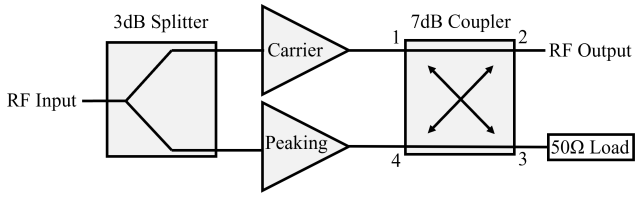

Fig. 1. Basic block diagram of the sequential power amplifier (SPA). The key differentiator of an SPA as compared to the Doherty is the output power combining without active load modulation.

Sequential power amplifiers (SPAs) are a potential alternative to the DPA for overcoming these challenges [7]–[9]. It is demonstrated that a carefully and deliberately designed SPA achieves wideband efficiency enhancement even at large OPBO [8]. Although similar to a DPA, it comprises of a carrier PA and peaking PA; however, unlike in a DPA, active load modulation using quarter-wave impedance transformers is dispensed with. Instead, power combining in a SPA occurs within a 50 Ω environment, crucial in facilitating its wideband operation and ease of design. The 50 Ω architecture further enables high modularity, 'plug-and-play' realisation with off-the-shelf components, re-configurable amplification and OPBO efficiency characteristics. This concept is preliminarily investigated in [8] by using PA evaluation boards and an in-house fabricated customised coupled-line combiner. However, the SPA of [8] is realized with SMA/3.5 mm connectors and the constituent PAs are not optimised for pinched-off operation. Moreover, because of its dual-input, it is required to manually determine the optimal relative phase between the carrier and the peaking PA inputs for maximum performance.

In this paper, a single-input SPA is proposed and the optimal phase shift is embedded within the hardware of the input splitter hence avoiding the need of requiring two RF modulators for the two inputs of [8]. The key contributions are as follows:

i. Optimal relative phase alignment is implemented inherent to the SPA components for leveraging the maximum possible drain efficiencies over a wide bandwidth.
ii. A quadrature hybrid coupler operating as a combiner is designed for deliberately optimising the power share between the carrier PA and peaking PA at the SPA output whilst maintaining the fractional bandwidth.

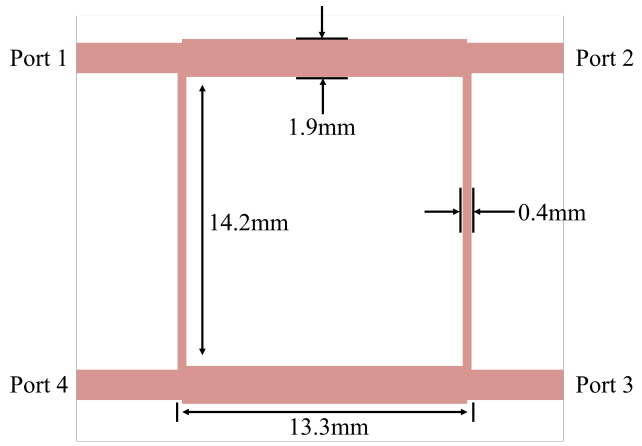

Fig. 2. Layout of the designed 7dB quadrature hybrid coupler operating as a combiner with port 3 terminated with a 50 Ω load.

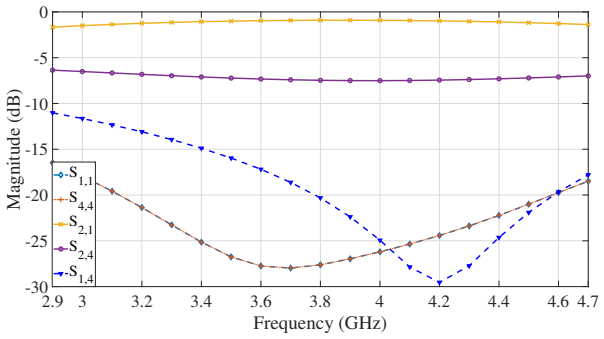

Fig. 3. The scattering parameters (S-parameters) of the quadrature hybrid combiner showing the coupling ratio and the isolation.

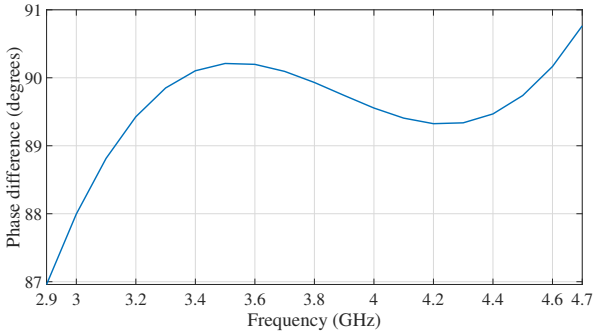

Fig. 4. Phase difference between the combiner's through path and coupling path ($S_{2,1}$ and $S_{2,4}$) to show the a relatively stable phase difference (around 90 degrees) that can be compensated with a transmission line.

iii. An input splitter is specially designed for streamlining the SPA architecture by driving it with a single RF power source.

To the best of the authors' knowledge, the achieved drain efficiency of ≈50 % over 1.8 GHz of bandwidth, with a maximum drain efficiency of 56 % at 3.5 GHz at the maximum output power and 52 % at 6 dB OPBO at the same frequency, is the best in comparison to the current state-of-the-art sequential PAs in literature.

II. SPA Design and Implementation

A. Carrier and Peaking PA Design

The SPA comprises of the carrier and peaking constituent PAs, a wilkinson splitter, and a quadrature hybrid combiner , as depicted in Fig. 1. The carrier PA is usually sized smaller than the peaking PA in order to ensure that the peak efficiency of the carrier PA is located around OPBO region of the peaking PA. However, in this work, the two constituent PAs are identically sized transistors of 10 W each (CG2H40010). The carrier PA is biased in class-AB for the linear operation of the SPA, whereas the peaking amplifier is biased in class-C for turn on with high input power levels. For the design of the PAs, a combination of high-efficiency continuous modes are used, as demonstrated in [10]. This combination of modes are class-J and continuous inverse class-F, which ensures that the best possible efficiency and bandwidth performance can be attained. These modes are achieved through the design of a filter for the output matching network using Keysight ADS' matching tool. This filter will then present the correct package impedances to the devices used, to achieve the desired combination of modes intrinsically within both devices. The same design is used for both the carrier and peaking PA. The drain voltage of the carrier PA is chosen to be 20 V which is lower than than the recommended voltage for the transistor (28 V) in order purposely saturate the carrier PA at a output lower power level as compared to the peaking PA, thus ensuring efficiency enhancement at large OPBO levels.

B. Design of Wideband Combiner

Designing a wideband combiner determines the overall wideband operation in a SPA. This is because the net bandwidth of the combiner should be equal to the overlapped band of operation of the constituent carrier and peaking PAs. The coupling ratio is another important aspect in the SPA operation. It is crucial for utilising the power from the carrier as well as the peaking PAs, since it dictates the power share from each of these constituent PAs at the output of the SPA. For example, a coupling ratio of 3 dB requires a 50 % power share from each of the constituent PAs at the SPA output; which also results in the loss of linear gain (at the SPA output (due to a corresponding sacrifice in linear gain at the carrier PA). A high coupling ratio of 10 dB, for instance, would utilise only 10 % of the power delivered from the peaking PA. Therefore, in our work, a coupling ratio of 7 dB is chosen so as to leverage up to 80 % of the SPA output power from the carrier PA and the remaining 20 % from the peaking PA. Albeit, targeting a coupling ratio of 7 dB using the traditional ways of combining signals can impose fabrication challenges such as in the case of coupled-line couplers where the coupled lines would need narrow spacing that is difficult to realise. Therefore, a quadrature hybrid combiner is implemented for attaining a targeted coupling ratio whilst maintaining bandwidth.

The combiner designed for this work, shown in Fig. 2, is a quadrature hybrid combiner. Fig. 3 shows the hybrid

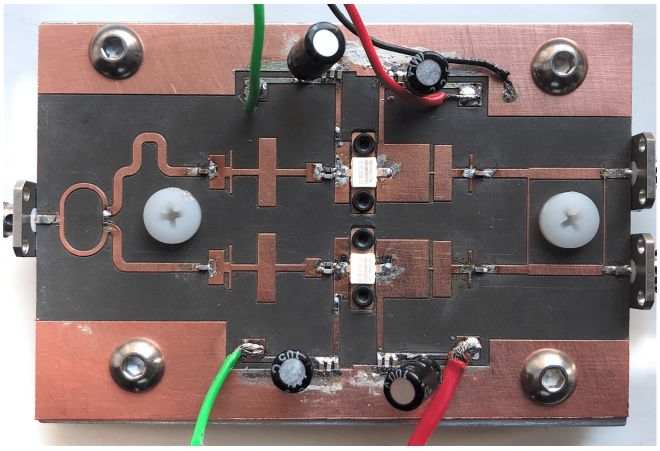

Fig. 5. Photo of the SPA protortpe showing the input splitter, the biased carrier and peaking PAs along with their associated matching circuits and the wideband combiner.

S-parameters and in particular the $S_{2,4}$ which effectively achieves the required 7 dB coupling ratio over the band of operation. Furthermore, the two input ports of the combiner (ports 1 & 4), being located on the adjacent side of the combiner, allows a direct feed for both the carrier and peaking PAs along with the additional ease of having 50 Ω load terminated on port 3 (which lies on the edge of the SPA board). However, if a coupled-line coupler is used, ports (3 & 4) would have swapped their locations bringing place-and-route difficulty in adding the 50 Ω termination in the middle of the SPA board; along with a longer feed required to reach port 4 from the peaking PA.

C. Optimal Relative Phase Compensation

The relative phase across the through and coupled paths in the combiner also has a significant impact on the SPA performance as it is the key for obtaining high drain efficiencies throughout the bandwidth of operation. Using quadrature hybrid combiner provides the required coupling ratio along with an optimal relative phase that would otherwise:

i. Either require a dedicated filter to shape the required phase response; or,
ii. Two dedicated RF inputs [8] where the phase at the input of one of the PAs is swept whilst the input phase at the other PA is held constant as a reference; thus creating a phase difference sweep to obtain the optimal relative phase across the bandwidth which maximises the SPA drain efficiency (optimal ϕ).

The combiner maintains a relative phase between the through path and the coupling path of about 90° ($\angle S_{2,1} - \angle S_{2,4} \approx 90°$) as shown in Fig. 4, which also allows for a feasible phase compensation by employing transmission lines inherent within the combiner (and the input splitter). In this way, our proposed SPA architecture removes the manual effort of determining the optimal relative phase ϕ between the carrier PA and the peaking PA (which is further swept over input powers) to extract the best achievable drain efficiencies.

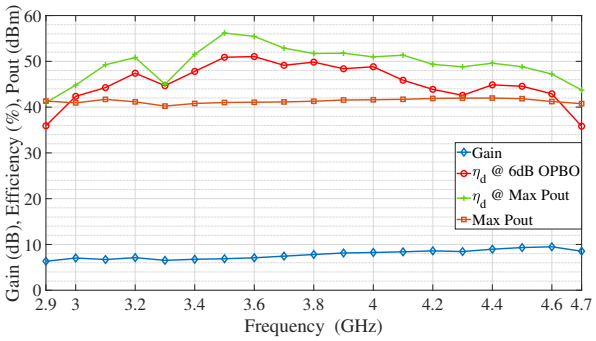

Fig. 6. Best possible drain efficiency (η_d) of the SPA at max. output power P_{out} and 6dB OPBO over the frequency of operation (2.9 GHz to 4.7 GHz, in steps of 100 MHz). Also shown are the gain and max. P_{out}. The fractional bandwidth of the SPA is $\frac{(4.7\,\text{GHz}-2.9\,\text{GHz})}{3.8\,\text{GHz}} = 47\,\%$.

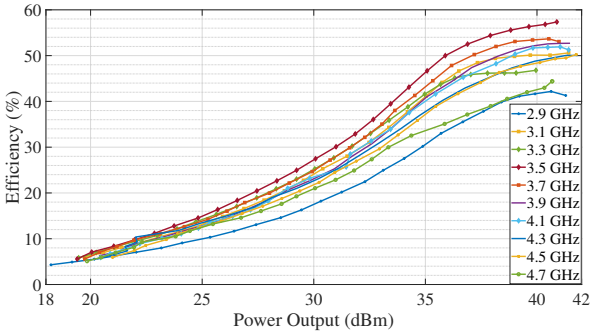

Fig. 7. Drain efficiencies of the SPA over swept output powers. Each trace represents a frequency between 2.9 GHz and 4.7 GHz with a step of 200 MHz.

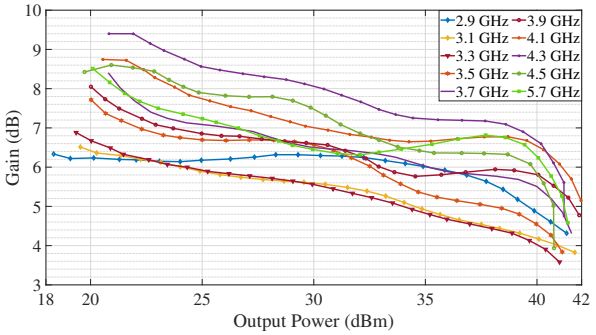

Fig. 8. The gain of the SPA over output power. Each trace represents a frequency between 2.9 GHz and 4.7 GHz with a step of 200 MHz.

III. Experimental Results

The schematic and layout for the SPA is shown in Fig. 5. Design effort is accomplished with Keysight ADS and fabricated in-house on Rogers RT/Duroid 5880 substrate of 0.508 mm thickness and 35 μm copper thickness. The SPA is biased with voltages of V_{GS}=-2.5 V and V_{DD}=20 V for the carrier PA; and with V_{GS}=-6 V and V_{DD}=34 V for the peaking PA. As stated previously in Section II, the V_{DD} for the carrier PA is kept lower than the recommended voltage of operation for the transistor so as to ensure OPBO power efficiency

TABLE I
COMPARISON OF THE PRESENTED SPA WITH OTHER STATE-OF-THE-ART PAS.

References	Type of PA Architecture	Frequency (GHz)	Fractional Bandwidth (%)	POUT, MAX (dBm)	Gain (dB)	OPBO (dB)	Drain Efficiency η_d @ Max Pout (%)	Drain Efficiency η_d @ OPBO (%)
[11] 2015	Single input SPA	2.0 - 3.0	40	39.7	10	5	26 - 37	33 - 61
[12] 2020	Single input SPA	1.5 - 2.4	46	42.3 - 44.3	12-15	6	50 - 63	40 - 45
[13] 2020	Envelope Tracking (ET) SPA	1.6 - 2.4	40	43.6	10-12	6	59	49-56
[14] 2019	3-stage DPA	1.6 - 2.6	47	45.5 - 46	10	6 - 9	53 - 66	50 - 63
[6] 2021	dual-frequency matching circuit	2.4 - 3.7	42	42 - 44.5	8-11	6	61.2 - 68.4	49.7 - 61.4
[15] 2018	2-way modified Doherty	1.35 - 2.05	41	41.5 - 42.4	11.8 - 14	9	53 - 66	50 - 53
[1] 2022	Sequential Load modulated Balanced Amplifier	1.8 - 2.75	37	44.6 - 45.8	10-12	8	60 - 68	51.8 - 69
This Work	Single input SPA	2.9 - 4.7	47	40-42	6.2-9.4	6	43-56	36-52

enhancement. The coupled port (port 3) of the combiner is terminated with a 50 Ω dummy load. This SPA demonstrates a remarkable bandwidth of 1.8 GHz while maintaining high backoff efficiency. This is achieved by using a quadrature hybrid combiner (as well as input splitter; with phase compensation being shared across both; in order to attain the optimal ϕ for delivering the highest possible drain efficiencies) instead of impedance transformers which can band-limit the SPA. Fig. 6 shows an attained bandwidth between 2.9 GHz and 4.7 GHz.

A drain efficiency (η_d) between 43 % - 56 % are measured at the peak output power across the bandwidth of 1.8 GHz; and measured drain efficiencies between 36 % - 52 % at 6 dB OPBO. Fig. 7 illustrates the drain efficiency curves over several swept output powers for frequencies ranging from 2.9 GHz to 4.7 GHz. Next, Fig. 8 shows the gain curves of SPA relative to output power for the same range of frequencies. Lastly, Table I summarises the performance of our proposed SPA as compared to the current state-of-the-art PAs.

IV. CONCLUSIONS

A single-input SPA with a 7 dB quadrature hybrid combiner and identically sized constituent PAs was implemented. The SPA components, i.e., the 7 dB wideband combiner and input splitter were designed considering the optimal relative phase ϕ between the through and coupled-paths for delivering the maximum possible efficiency over the band of operation. Measurement results demonstrated hitherto the best achieved drain efficiencies in its class over a wide bandwidth of operation, making this SPA suitable to replace multiple PAs in a base-station transmitter.

REFERENCES

[1] C. Chu, T. Sharma, S. K. Dhar, R. Darraji, X. Wang, J. Pang, and A. Zhu, "Waveform engineered sequential load modulated balanced amplifier with continuous class-f- 1 and class-j operation," *IEEE Transactions on Microwave Theory and Techniques*, vol. 70, no. 2, pp. 1269–1283, 2021.

[2] T. Cappello, P. Pednekar, C. Florian, S. Cripps, Z. Popovic, and T. W. Barton, "Supply-and load-modulated balanced amplifier for efficient broadband 5g base stations," *IEEE Transactions on Microwave Theory and Techniques*, vol. 67, no. 7, pp. 3122–3133, 2019.

[3] T. Barton, "Not just a phase: Outphasing power amplifiers," *IEEE Microwave Magazine*, vol. 17, no. 2, pp. 18–31, 2016.

[4] B. Kim, J. Kim, I. Kim, and J. Cha, "The doherty power amplifier," *IEEE microwave magazine*, vol. 7, no. 5, pp. 42–50, 2006.

[5] X. Y. Zhou, W. S. Chan, J. Pang, J. Xia, and W. Feng, "Broadband doherty-like power amplifier using paralleled right-and left-handed impedance transformers," *IEEE Transactions on Microwave Theory and Techniques*, vol. 68, no. 11, pp. 4599–4610, 2020.

[6] J. Nan, H. Wang, M. Cong, and W. Yang, "A Broadband Doherty Power Amplifier With a New Load Modulation Network," *IEEE Access*, vol. 9, pp. 58 025–58 033, 2021.

[7] S. C. Cripps, *RF Power Amplifiers for Wireless Communications*. Artech house Norwood, MA, 2006, vol. 2.

[8] S. Ozan, M. Nair, M. A. Beach, and T. Cappello, "Modular design and characterization of a reconfigurable sequential power amplifier," in *2022 IEEE 22nd Annual Wireless and Microwave Technology Conference (WAMICON)*. IEEE, 2022, pp. 1–4.

[9] T. Lehmann and R. Knoechel, "Design and performance of sequential power amplifiers," in *2008 IEEE MTT-S International Microwave Symposium Digest*. IEEE, 2008, pp. 767–770.

[10] A. Pitt, T. Cappello, and K. Morris, "Combining class j and inverse class f continuous modes for a highly efficient broadband power amplifier," in *European Microwave Conference*, 2022.

[11] J. Shao, R. Ma, K. H. Teo, S. Shinjo, and K. Yamanaka, "A fully analog two-way sequential gan power amplifier with 40% fractional bandwidth," in *2015 IEEE International Wireless Symposium (IWS 2015)*. IEEE, 2015, pp. 1–3.

[12] P. Chen, R. Quaglia, J. Lees, B. M. Merrick, A. Alt, and P. J. Tasker, "Look-up table method for optimising coupling ratio in broadband sequential power amplifiers," *IET Microwaves, Antennas & Propagation*, vol. 14, no. 13, pp. 1626–1634, 2020.

[13] ——, "Efficiency enhancement of a broadband sequential power amplifier using envelope tracking," in *2020 International Workshop on Integrated Nonlinear Microwave and Millimetre-Wave Circuits (INMMiC)*. IEEE, 2020, pp. 1–3.

[14] J. Xia, W. Chen, F. Meng, C. Yu, and X. Zhu, "Improved three-stage doherty amplifier design with impedance compensation in load combiner for broadband applications," *IEEE Transactions on Microwave Theory and Techniques*, vol. 67, no. 2, pp. 778–786, 2018.

[15] X.-H. Fang, H.-Y. Liu, K.-K. M. Cheng, and S. Boumaiza, "Modified doherty amplifier with extended bandwidth and back-off power range using optimized peak combining current ratio," *IEEE Transactions on Microwave Theory and Techniques*, vol. 66, no. 12, pp. 5347–5357, 2018.